

Rotor Flow Analysis using Animplicit Harmonic Balance Method

D. Im, S. Choi, H. Kwon, S. H. Park and J. H. Kwon

Abstract—This paper is an extension of a previous work where a diagonally implicit harmonic balance method was developed and applied to simulate oscillatory motions of pitching airfoil and wing. A more detailed study on the accuracy, convergence, and the efficiency of the method is carried out in the current paper by varying the number of harmonics in the solution approximation. As the main advantage of the method is its usage for the design optimization of the unsteady problems, its application to more practical case of rotor flow analysis during forward flight is carried out and compared with flight test data and time-accurate computation results.

Keywords—Design optimization, Implicit harmonic balance method, number of harmonics, rotor flows

I. INTRODUCTION

An implicit harmonic balance method was developed in the previous study. The method was applied to predict the simple oscillatory motions of pitching airfoil and wing, and was compared with the experiments and the time-accurate computation results [1]. The convergence of the flow solution was investigated with respect to the different number of harmonics used in the solution approximation.

On the other hand, a similar nonlinear frequency domain-based method, a Time-Spectral approach, was developed and applied to simulate the more practical case of helicopter rotor flow analysis for steady level forward flight [2-4]. A wide range of forward flight regime was simulated with good agreements with flight data and time-accurate computation results. A design aspect of the time-spectral method for the rotor blades was also investigated at level forward flight in combination with the state-of-the-art adjoint solution method [5].

Although identical in the central idea of approximating the solutions by Fourier series, the harmonic balance method is different from the time-spectral method in the treatment of the periodic boundary conditions and the application of FFT directly in the solution procedure. [6-7]

A computational efficiency of the harmonic balance

method can be higher due to the implicit treatment of the spectral operator terms in the formulation. An application of the periodic boundary conditions in space and time can further improve computational efficiency by reducing a computational domain to contain only one blade of the rotor [4]. A main purpose of the present study is to investigate the accuracy and efficiency of the harmonic balance method in the rotor flow analysis. The magnitude of the oscillations in the pitching motions simulated in the previous study were limited to be small, and the waveforms of the resulting force components were smooth in shape. Thus a small number of harmonics in the Fourier series approximation of the solutions were shown to be sufficient in the accurate prediction of the flow solutions. However, in forward flight, dynamic stall phenomena are occurring during forward flight in the retreating side of the rotor disc. The waveforms of the corresponding sectional force components can be non-smooth and contains higher harmonics components in the frequency domain. Thus, dynamic stall conditions of the pitching motions of such airfoils as SC1095 and NACA0015 are simulated in the current study using harmonic balance method with varying number of harmonics in the solution approximation. Those airfoils are used in the existing helicopter rotors of UH-60A and the active flap model rotor, and the experimental data are available in Reference [8-9]. It should also be noted that any frequency-based analysis method does not include an explicit time derivative term in the formulation and has a great potential in the design optimization of the periodic unsteady problems. A sensitivity analysis of the unsteady problems can be carried out by using a powerful adjoint solution technique, which can be easily implemented in the steady formulation of the governing equation in the harmonic balance method. In fact, a time-spectral and adjoint-based design method was developed and applied to design a rotor blade shape of UH-60A Blackhawk helicopter. An ultimate goal of the current work is the application of the harmonic balance method to the rotor blade design during forward flight. The current study is a preliminary work of validation of the method to be applied in the rotor flow analysis, and the design aspects of the method will be carried out in a near future. The organization of the paper is as follows: a brief introduction of the problem formulation is shown in section II. Aspects of the accuracy, convergence and the computational efficiency of the method is demonstrated in section III by taking an example of the two pitching airfoils. Finally, rotor flow analysis at both hovering and non-lifting forward flight condition is presented.

D. Im, Ph. D. Candidate, Dept. of Aerospace Engineering, Korea Advanced Institute of Science and Technology (e-mail: im1304@kaist.ac.kr).

S. Choi, Assistant Professor, Dept. of Aerospace Engineering, Korea Advanced Institute of Science and Technology, S. Korea (e-mail: schoi1@kaist.ac.kr).

H. Kwon, Ph. D. Candidate, Dept. of Aerospace Engineering, Korea Advanced Institute of Science and Technology (e-mail: aero382@kaist.ac.kr).

S. H. Park, Assistant Professor, Dept. Aerospace Information Engineering, S. Korea (e-mail : pish@konkuk.ac.kr)

J. H. Kwon, Professor, Dept. of Aerospace Engineering Korea Advanced Institute of Science and Technology, S. Korea (e-mail: jhkwon@kaist.ac.kr).

II. FORMULATION

To derive the governing equations of the frequency domain techniques, the general time domain governing equations are presented as Eq. (1):

$$F(t) = \frac{dQ(t)}{dt} + R(t) = 0 \quad (1)$$

The residual R and solution Q are assumed to be periodic in the time domain, and R and Q can respectively be expressed as Eq. (2) and Eq. (3) in a Fourier series with the finite number of harmonics:

$$Q(t) = \hat{Q}_0 + \sum_{n=1}^{N_H} (\hat{Q}_{cn} \cos(\omega n t) + \hat{Q}_{sn} \sin(\omega n t)) \quad (2)$$

$$R(t) = \hat{R}_0 + \sum_{n=1}^{N_H} (\hat{R}_{cn} \cos(\omega n t) + \hat{R}_{sn} \sin(\omega n t)) \quad (3)$$

$$F(t) = \hat{F}_0 + \sum_{n=1}^{N_H} (\hat{F}_{cn} \cos(\omega n t) + \hat{F}_{sn} \sin(\omega n t)) \quad (4)$$

In Eq. (2), the Fourier coefficients of conservative variables are not functions of time, and by substituting Eq. (2) and Eq. (3) into Eq. (1) the governing equations represent the relationships of the Fourier coefficients. A comparison of Eq. (4) and the governing equations expressed as Eq. (5) in the form of a matrix:

$$\omega M \hat{Q} + \hat{R} = 0 \quad (5)$$

The M matrix ($N_T (= 2N_H + 1) \times N_T$) is a $M(n+1, N_H + n + 1) = n$, $M(N_H + n + 1, n + 1) = -n$ and the other value is 0. \hat{Q} and \hat{R} in Eq. (5) are arranged as shown in Eq. (6) and Eq. (7):

$$\hat{Q} = (\hat{Q}_0, \hat{Q}_{c_1}, \hat{Q}_{c_2}, \dots, \hat{Q}_{c_{N_H}}, \hat{Q}_{s_1}, \hat{Q}_{s_2}, \dots, \hat{Q}_{s_{N_H}})^T \quad (6)$$

$$\hat{R} = (\hat{R}_0, \hat{R}_{c_1}, \hat{R}_{c_2}, \dots, \hat{R}_{c_{N_H}}, \hat{R}_{s_1}, \hat{R}_{s_2}, \dots, \hat{R}_{s_{N_H}})^T \quad (7)$$

Here, for a non-linear relationship for \hat{Q} and \hat{R} , it is very difficult to solve Eq. (5) directly. Using the method proposed by Hall [10] Eq. (5) transformed in the time domain by the Fourier series. Eq. (5) represents Eq. (11) using the sub-time level ($\Delta t = 2\pi / (N_T \omega)$) of the cycle ($T = 2\pi / \omega$), as the Fourier transform represented as Eq. (8) and Eq. (9):

$$\hat{Q} = \mathfrak{I} Q_{hb} \quad (8)$$

$$\hat{R} = \mathfrak{I} R_{hb} \quad (9)$$

The Fourier coefficient terms (\hat{Q}, \hat{R}) in the Eq. (5) is substituted by Eq. (8) and (9). It is also rearranged as Eq. (10). To facilitate the flux term computation, the inverse Fourier transform is multiplied:

$$\omega M \mathfrak{I} Q_{hb} + \mathfrak{I} R_{hb} = \omega \mathfrak{I}^{-1} M \mathfrak{I} Q_{hb} + \mathfrak{I}^{-1} \mathfrak{I} R_{hb} = 0, \quad (10)$$

$$\omega D Q_{hb} + R_{hb} = 0 \quad (11)$$

where $D (= \mathfrak{I}^{-1} M \mathfrak{I})$ is the spectral operator in Eq. (11). By applying pseudo-time stepping in Eq. (11), the harmonic balance method can be expressed in its final form [11]:

$$\frac{dQ_{hb}}{d\tau} + R_{hb} + \omega D Q_{hb} = 0 \quad (12)$$

A. Flow solver

The dual-time stepping method for a time-accurate unsteady solution was used, and the diagonalized ADI method was used for pseudo-time iterations to obtain a steady-state solution at each time-step [12-13]. For the explicit harmonic balance method, the fourth-order R-K (Runge-Kutta) integration was employed. The proposed harmonic balance method was applied in the time-domain method, which uses the diagonalized ADI method. Each spatial numerical flux was discretized using Roe's FDS scheme. To obtain higher accuracy, the third-order MUSCL scheme was applied. The turbulent eddy viscosity was computed from the two-equation $k - \omega$ Wilcox-Durbin+ turbulence model [14].

III. ACCURACY, CONVERGENCE AND EFFICIENCY

In the previous study, pitching motions of both two-dimensional airfoil and three-dimensional wing were limited to the small oscillations so that flow streams were fully attached over the surfaces without major flow separations observed in the solution [1]. Resulting waveforms of aerodynamic force components are smooth enough for the method to accurately predict the flows with only a small number of harmonics. However, rotor flows experience dynamic stall during forward flight in the retreating side of the rotor disk, a dynamic stall phenomenon is simulated in this section. Mach number is $M = 0.29$, and Reynolds number $Re = 1.951 \times 10^6$ based on the chord length. The reduced frequency is $F^+ = 0.096$, which amount to the natural frequency $\omega = 63.7$. A pitching amplitude is $\Delta\alpha = 4.16^\circ$, while the mean amplitude is $\alpha_0 = 15^\circ$. The periodic pitching motion, $\alpha(t)$, is approximated by sine function, $\alpha(t) = \alpha_0 + \Delta\alpha \cdot \sin(\omega t)$ [9]. The mesh topology for this calculation is shown in Figure 1. A C-type mesh is generated with 129 points along the wake region, 259 points in circumferential direction of the airfoil, and 129 points in the normal direction to the surface ($Y+ \sim 1$).

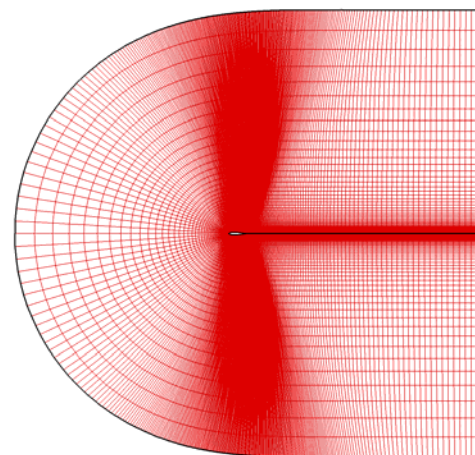


Fig. 1 C-type computational mesh topology around NACA0015 airfoil (513 X 129 mesh points)

B. Accuracy and convergence

To investigate the accuracy and the convergence of the present harmonic balance method, the number of harmonics in

the method varies from 5 to 17. The resulting aerodynamic force components of C_l , C_d and C_m are plotted in Figure 2, 3 and 4 respectively, and compared with the experimental data as well as the time-accurate computations. Unlike the pitching motions of NACA0012 airfoil in the previous study where excellent agreements with experiments were shown for all cases, certain amounts of discrepancies are present in the current dynamic stall simulation. That is not surprising considering the well-known limitations of Reynolds Averaged Navier-Stokes solver with turbulence models for the prediction of the massive separation regions of dynamic stall. However, good convergence histories are observed in L2 norm of density residual in Figure 5 and 6 regardless of the number of harmonics. A total number of harmonics of 9 or higher appear to converge well and show good agreements with time-accurate computation results. A minimum number of harmonics to provide a required accuracy is determined by investigating the frequency contents of the waveform as in Figure 7 and 8. Components higher than 4 harmonics nearly vanish in lift coefficient and 7 harmonics in drag coefficient. This reconfirms the convergence shown in Figure 2, 3 and 4 for harmonics higher than 7.

C. Computational efficiency

An efficiency of computational time saving is plotted in Figure 5 and 6 with respect to the varying number of harmonics. A comparison of convergence in Figure 6 indicates that a harmonic balance method with the multigrid acceleration approach is three times faster than the one without multigrid scheme. Also the harmonic balance computation with the multigrid is almost twenty times faster than the explicit computations. A dependence of the convergence on the varying number of harmonics is not obvious and the similar convergence rates are shown for different number of harmonics.

A computational efficiency with the different number of harmonics is a critical factor to determine a minimum number of harmonics to guarantee the required accuracy. A numerical test to vary the number of harmonics and measure total wall-clock CPU time in converging the solutions at the given accuracy level is carried out and plotted in Figure 7 in comparison with the linear curve for a reference. A linear increase in time is observed with the number of harmonics in present method, but in another frequency domain method, the effect of a quadratic increase is gradually observed as the number of harmonics increases.

This is because the computation of an additional spectral derivative term involves a multiplication of a matrix and a vector, which is a linear order. [4] Therefore, the choice of the number of harmonics in the harmonic balance method is sensitive to the frequency contents of the original waveform to reconstruct, thus its accuracy and efficiency can be compromised depending on the smoothness of the waveforms.

TABLE I
 COMPARISON OF COMPUTATION TIME

Computation method	Computation time (in seconds)
Time-accurate method with 0.7° time step	15247
Harmonic balance method with 10 harmonics	3477

However, it has been demonstrated that the number of harmonics up to 25 appears to be sufficient to predict the flow solutions even at the moderate stall cases at the efficiency better than that of the time-accurate computation.

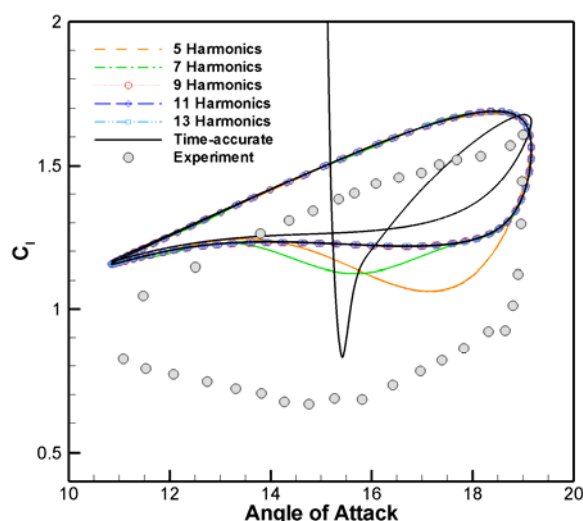


Fig. 2 Comparison of C_l values with respect to the varying number of harmonics (pitching NACA0015 airfoil)

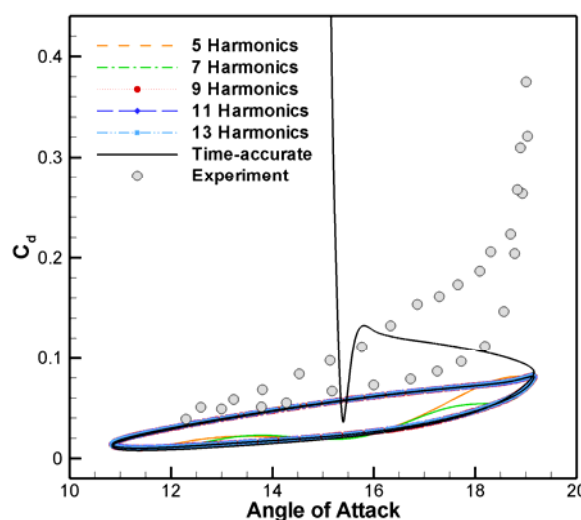


Fig. 3 Comparison of C_d values with respect to the varying number of harmonics (pitching NACA0015 airfoil)

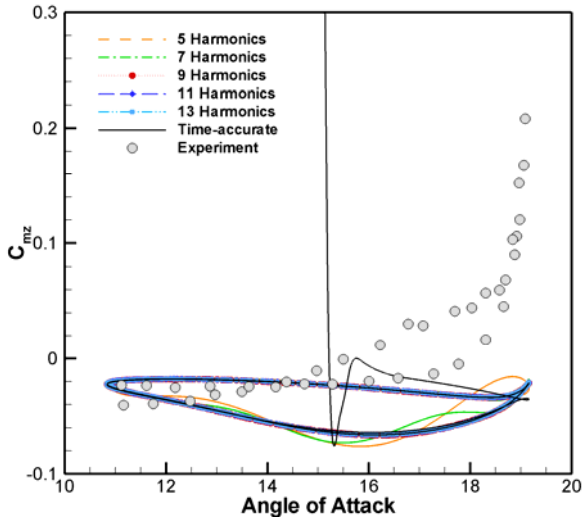


Fig. 4 Comparison of C_m values with respect to the varying number of harmonics

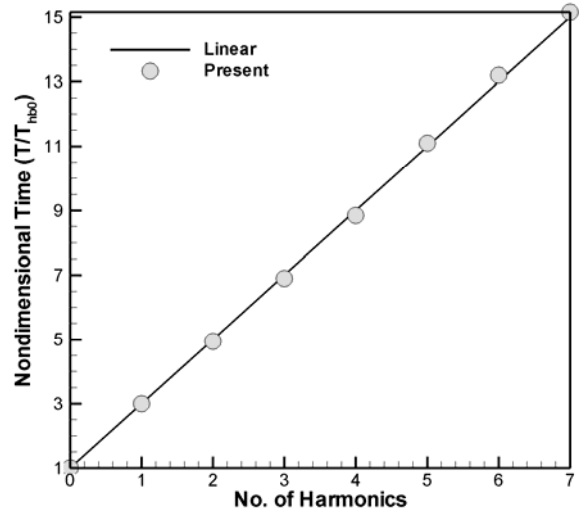


Fig. 7 Computation time with respect to the number of harmonics

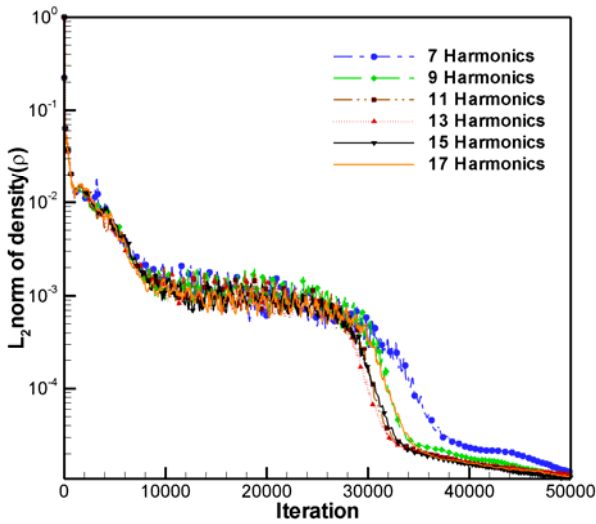


Fig. 5 Convergence history of L_2 norm of density residual with respect to varying number of harmonics

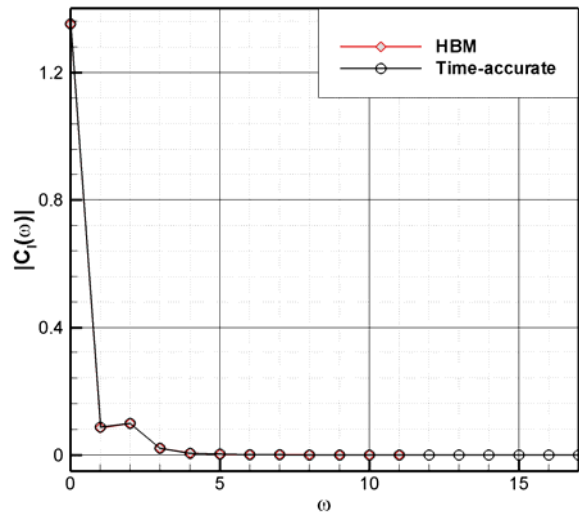


Fig. 8 Frequency contents of lift coefficient (C_l)

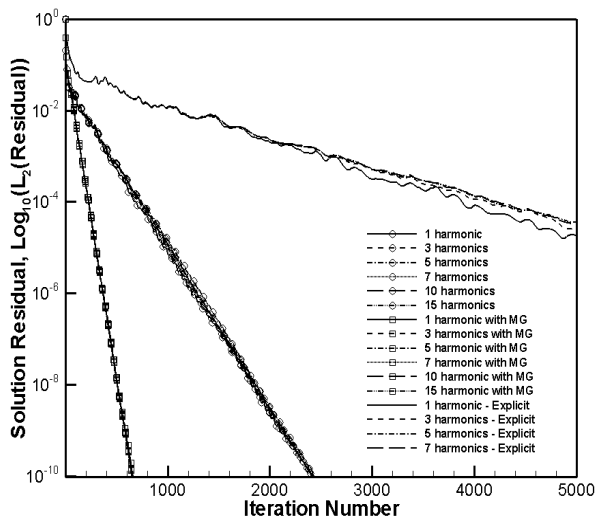


Fig. 6 Comparison of convergences of harmonic balance methods with varying number of harmonics

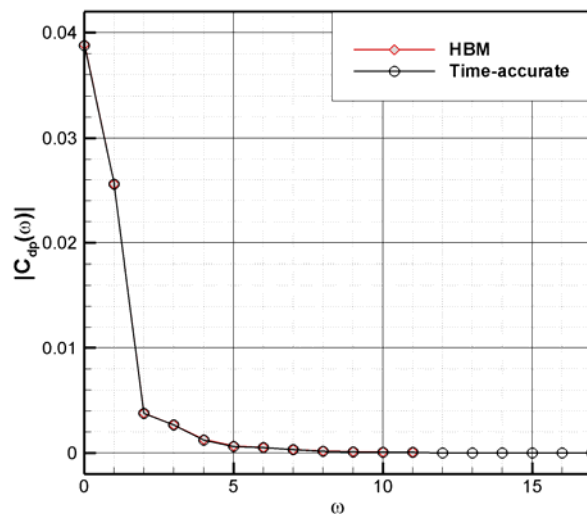


Fig. 9 Frequency contents of pressure drag coefficient (C_{dp})

IV. TEST CASES

As a preliminary study to apply the proposed harmonic balance method to the rotor flow analysis and design, a various range of rotor flows is simulated: a dynamic stall of pitching airfoil, and hovering and non-lifting forward flights of the helicopter rotors.

D. Pitching motions of SC1095 Airfoil

As SC1095 airfoil is used in the UH-60A Blackhawk helicopter, it was chosen for the dynamic stall simulation. Reduced frequency, $F_+ = 0.1$, Mach number, $M = 0.3$, and Reynolds number, $Re = 3.7 \times 10^6$. A Pitching motion is described as $\alpha(t) = 10 + 10 \sin(\omega t)$. Computation results of both time-accurate and harmonic balance computations are shown in Figure 10 and 11, and demonstrate reasonable agreements with the experiments. However, the harmonic balance results do not show excellent agreements with time-accurate results, which can be explained by the higher harmonic components in the frequency contents of C_l and C_d curves shown in Figure 12 and 13. Frequency contents of C_l and C_d are constructed by applying a Fast Fourier Transform (FFT) in the time-accurate results with reasonably small time step of 0.03125^0 . Unlike the pitching motions of NACA0015 airfoil shown in Figure 8 and 9, higher harmonics in the frequency contents are present in the wide range of high frequency region, thus the accuracy of the harmonic balance can be achieved with rather a large number of harmonics in the solution approximation. The number of harmonics as many as 25 is used for the harmonic balance computation to simulate the dynamic stall case of SC1095 airfoil. Even with 25 harmonics in the computation, the agreement of flow solution is not as good as in the pitching NACA0015 airfoil, and the effects of the aliasing errors are shown in Figure 12 and 13 to be still non-negligible even with 60 harmonics. In fact, a harmonic balance computation with the number of harmonics more than 25 is currently carried out and will be presented in the full paper.

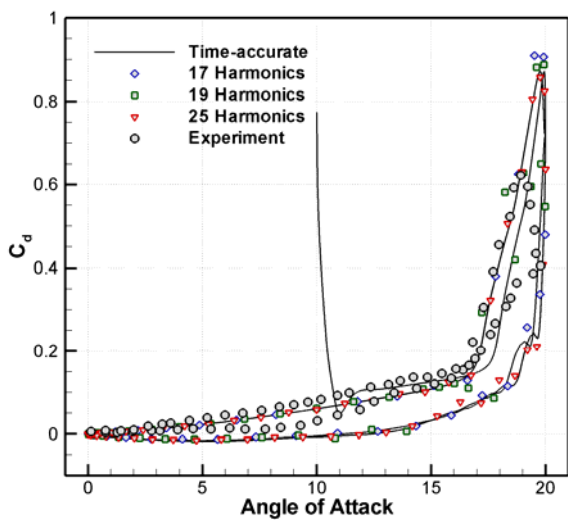


Fig. 10 Comparison of the drag coefficient prediction in pitching motion of SC1095 airfoil

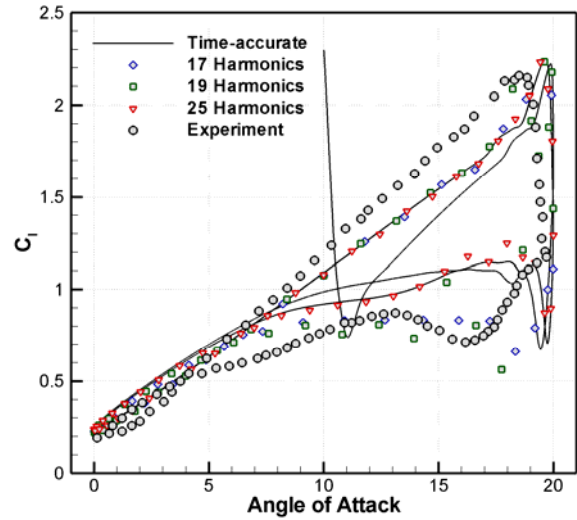


Fig. 11 Comparison of lift coefficient prediction in the pitching motion of SC1095 airfoil

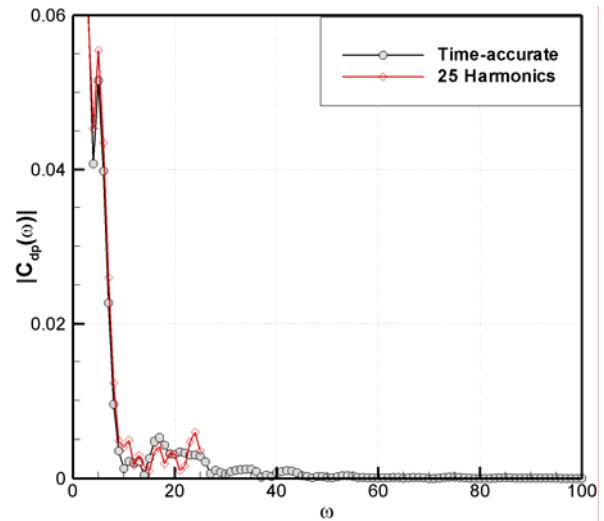


Fig. 12 Frequency contents of drag coefficient

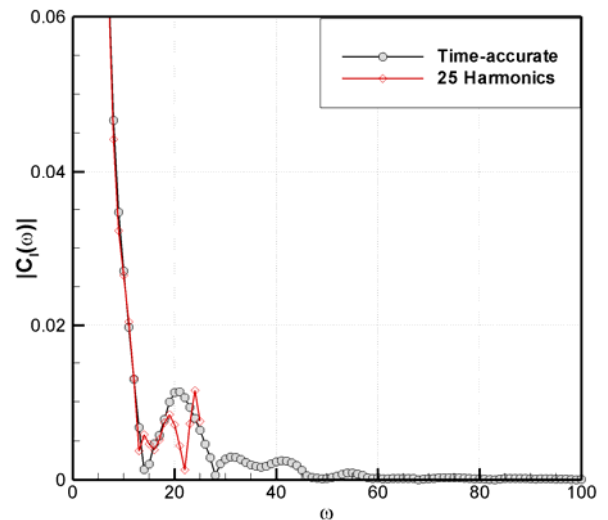


Fig. 13 Frequency contents of lift coefficient

E. Helicopter rotor in hovering

As a more practical application of the proposed harmonic balance method to the rotor flow analysis, both hovering and the forward flight of three-dimensional helicopter rotor are simulated. The two-bladed Caradona-Tung rotor is used for both flight conditions, as the wind tunnel test data are available for the comparison. The rotor blades do not have twist and are set at the collective pitch angle of 8° . For the hovering case, wind-tunnel test data with two tip Mach numbers are available, $M_{tip}=0.439$ and 0.877 cases. Although both cases are analyzed in the current study, results from the transonic flow conditions are presented in the paper. Although a single blade with steady computation is enough for the hovering computation, the harmonic balance with three harmonics is used for the hovering simulation just to test out the applicability of the current method to the three-dimensional rotor flows.

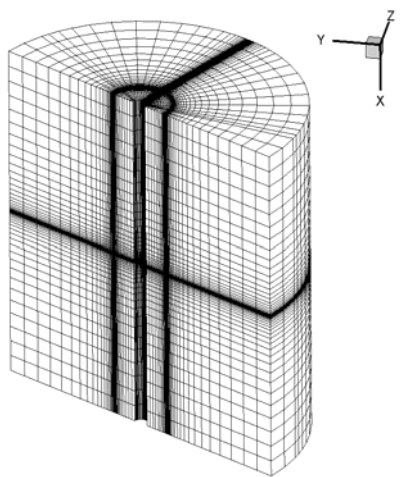


Fig. 14 Computational mesh topology for Caradona and Tung model (33x57x113)

Pressure coefficients over the cross sectional airfoils at the four spanwise locations of $r/R = 68, 80, 89,$ and 96% are plotted in Figure 15 and compared with the experimental data and the time-accurate computation results. Towards a blade tip area, a transonic shock is formed on the upper surface of the airfoil. Although small amount of discrepancies are present between the experiments and the time-accurate results, especially in the deceleration region of the upper surface around the transonic shock region, excellent agreements are shown between the time-accurate computations and the harmonic balance results with different number of harmonics.

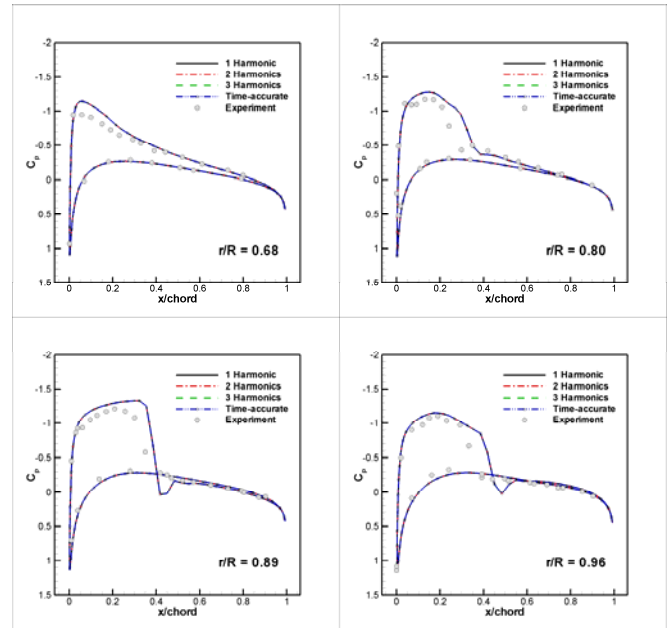


Fig. 15 Pressure coefficients at the four span locations of the rotor blade, hovering flight with $M=0.877$

A. Helicopter rotor in forward flight

A second test case of the rotor simulation is for the similar blades but at the non-lifting forward flight conditions. A rotor with the rectangular blades with no twist and no collective pitch angle is used. A tip Mach number, $M=0.8$

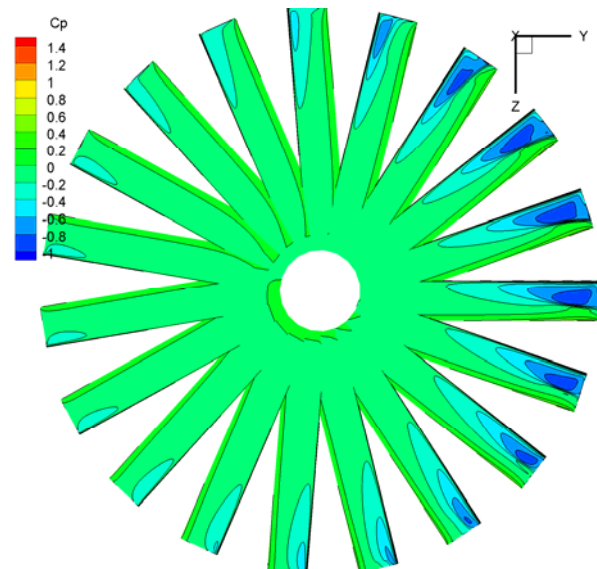


Fig. 16 Pressure contour plot of non-lifting forwarding flight using 9 harmonics

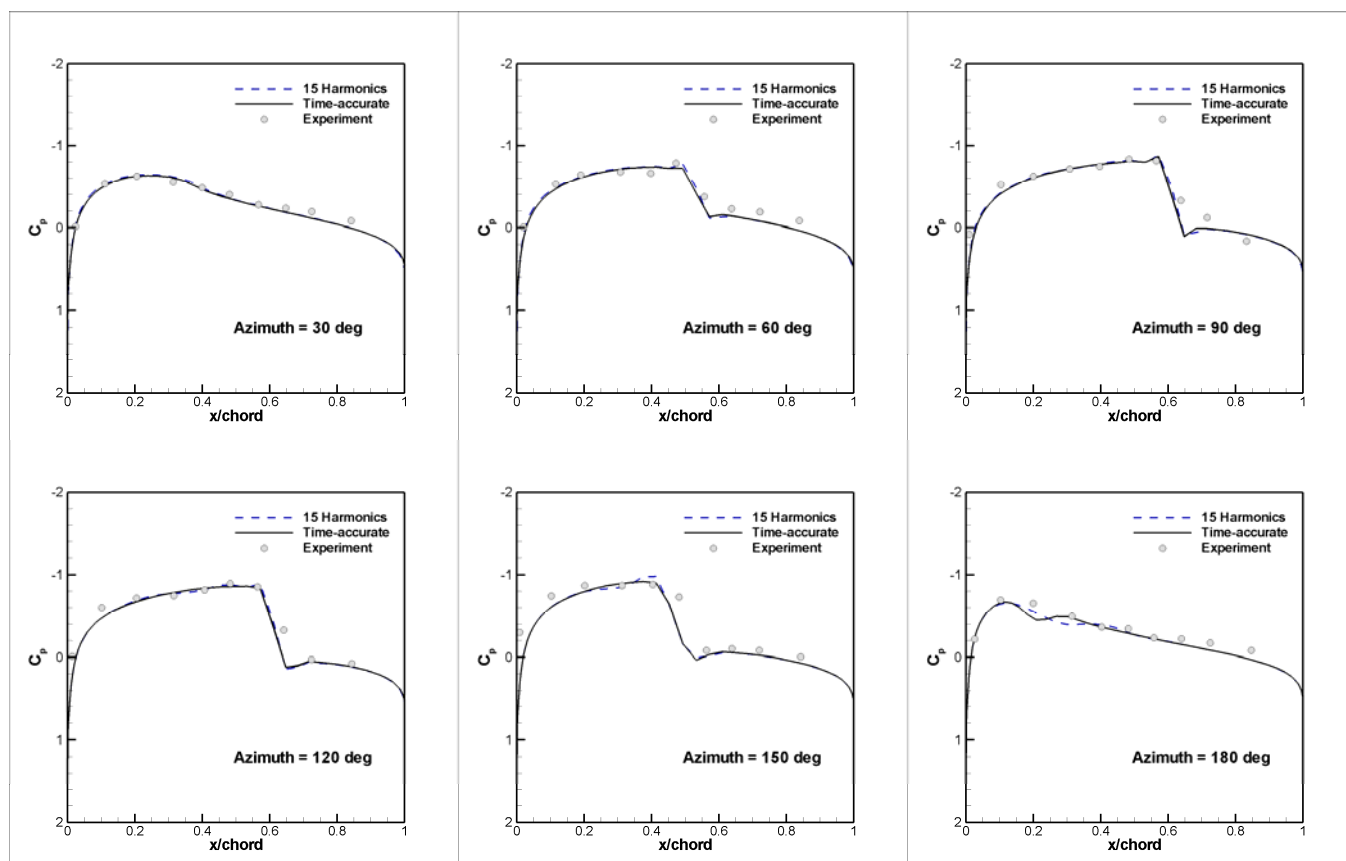


Fig. 17 Pressure coefficients at the six span locations of the rotor blade, forward speed of $M_{tip}=0.8$ and the advance ratio, $\mu = 0.2$

REFERENCES

- [1] Im, D., Kwon, J. H., and Park, S. H., "Periodic Unsteady Flow Analysis Using a Diagonally Implicit Harmonic Balance Method", submitted to the AIAA Journal, Jan. 2011
- [2] Choi, S., and Datta, A., "CFD Prediction of Rotor Loads Using Time-Spectral Method and ExactFluid-Structure Interface", 26th AIAA Applied Aerodynamics Conference, Aug. 2008, Honolulu, Hawaii.
- [3] Choi, S., and Datta, A., "CFD Prediction of Rotor Loads Using Time-Spectral Method and ExactFluid-Structure Interface", (accepted for Journal of American Helicopter Society, under revision.)
- [4] Ekici, K., Hall, K.C. and Dowell, E.H., "Computationally Fast Harmonic Balance Methods for Unsteady Aerodynamic Predictions of Helicopter Rotors," Journal of Computational Physics, Vol.227, 2008, pp. 6206-6225
- [5] Choi, S., Potsdam, M., Lee, K., Iaccarino, G., and Alonso, J. J., "Helicopter Rotor Design Using a Time-Spectral and Adjoint-Based Method", 12th AIAA/ISSMO Multidisciplinary Analysis and Optimization Conference, Sep. 2008, British Columbia, Canada.
- [6] Gopinath, A.K. and Jameson, A., "Time Spectral Method for Periodic Unsteady Computations over Two- and Three- Dimensional Bodies," 43rd AIAA Aerospace Sciences Meeting and Exhibit, AIAA Paper 2005-1220, Reno, NV, January 10-13, 2005.
- [7] McMullen, M., Jameson, A., and Alonso, J., "Demonstration of Nonlinear Frequency Domain Methods," AIAA Journal Vol.44, No.7, 2006, pp. 1428-1435
- [8] Dawson, S., Marcolini, M., Booth, E., Straub, F. K., Hassan, A. A., Tadghighi, H. and Kelly, H., "Wind Tunnel Test of An Active Flap Rotor: BVI Noise and Vibration Reduction," paper presented at the 51st Annual Forum of the American Helicopter Society, May 1995.
- [9] A. R. Piziali "An experimental investigation of 2D and 3D oscillating wing aerodynamics for a range of angles of attack including stall," NASA TM 4632, 1994
- [10] Hall, K.C., Thomas, J.P., and Clark, W.S., "Computation of Unsteady Nonlinear Flows in Cascades Using a Harmonic Balance Technique," AIAA Journal, Vol. 40, No. 5, 2002, pp. 879-886.
- [11] Thomas, J.P., Custer, C.H., Dowell, E.H. and Hall, K.C., "Unsteady Flow Computation Using a Harmonic Balance Approach Implemented about the OVERFLOW 2 Flow Solver," 19th AIAA Computational Fluid Dynamics Conference, AIAA Paper 2009-4270, San Antonio, TX, June, 2009.
- [12] Pulliam, T.H. and Chaussee, D.S., "A Diagonal Form of an Implicit Approximate-Factorization Algorithm," Journal of Computational Physics, Vol.39, 1981, pp. 347-363
- [13] Jameson, A., "Time Dependent Calculations Using Multigrid with Applications to Unsteady Flows Past Airfoils and Wings," AIAA 10th CFD Conference, AIAA Paper 91-1596, June, 1991
- [14] Park, S.H. and Kwon, J.H., "Implementation of Turbulence Models in an Implicit Multigrid Method," AIAA Journal, Vol.42, No.7, 2004, pp. 1348-1357